

Photo-Cross-Linking between Polymers Derivatized with Photoreactive Ruthenium–1,4,5,8-Tetraazaphenanthrene Complexes and Guanine-Containing Oligonucleotides

Stéphanie Deroo,[†] Veska Toncheva,[‡] Eric Defrancq,[§] Cécile Moucheron,[†]
Etienne Schacht,^{*,‡} and Andrée Kirsch-De Mesmaeker^{*,†}

Organic Chemistry and Photochemistry, Université Libre de Bruxelles, CP 160/08, 50 Avenue F. D. Roosevelt, 1050 Brussels, Belgium, Polymer Materials Research Group, Organic Chemistry, University of Ghent, 281 Krijgslaan, 9000 Ghent, Belgium, and Département de Chimie Moléculaire, UMR CNRS 5250, Université Joseph Fourier, BP 53, 38041 Grenoble Cedex 9, France

Received June 10, 2007; Revised Manuscript Received August 29, 2007

We have shown previously that complexes containing 1,4,5,8-tetraazaphenanthrene (TAP) ligands are able to form photoadducts with the guanine bases of DNA and oligonucleotides. In this work, we have exploited this specific photoreaction for carrying out photo-cross-linkings between guanine-containing oligonucleotides (G-ODNs) and biodegradable polymers derivatized with the photoreactive Ru(II) compounds. The aim in the future is to use these polymer conjugates as vectorizing agents of the metallic compounds inside the cells. Thus, photooxidizing Ru(II) complexes such as $[\text{Ru}(\text{TAP})_3]^{2+}$ and $[\text{Ru}(\text{TAP})_2\text{phen}]^{2+}$ (phen = 1,10-phenanthroline) have been derivatized by an oxyamine function to attach them, via an oxime ether linkage, to a soluble 6 or 80 kDa poly-[N-(2-hydroxyethyl)-L-glutamine] polymer that contains pendent aldehyde groups. It is demonstrated that the resulting Ru-labeled polymers exhibit photophysical properties and a photochemistry that are comparable with those of the free, nonattached complexes. The photo-cross-linkings with the G-ODNs are clearly detected by gel electrophoresis with the 6 kDa Ru conjugates upon illumination.

Introduction

Transition metal complexes have been extensively studied as probes of nucleic acids or metal-based drugs over the last two decades.^{1–3} In this context, the effects of nucleic acids on the photophysics and photochemistry of Ru(II) complexes have been the subject of intensive research.^{4,5} More particularly, it has been shown by our team that excited ruthenium(II) complexes bearing at least two 1,4,5,8-tetraazaphenanthrene (TAP) ligands are able to abstract an electron from the guanine (G) residues of mononucleotides (guanosine-5'-monophosphate, GMP), synthetic oligodeoxyribonucleotides (ODNs), or natural DNA.⁶ This photoelectron transfer process can lead to different reactions such as guanine oxidation,⁷ cleavage of the DNA backbone,⁸ and most interestingly irreversible photoadduct formation between the complex and the G residues.^{9–11} Indeed the presence of this photoadduct has been shown to block in vitro the function of RNA polymerase with DNA templates.¹² Such complexes that are biologically photoactive are considered as novel interesting potential drugs because their activity offers the advantage, over that of classical transition metal-based drugs, to be triggered only under illumination.¹³ Although the in vitro results with the TAP complexes are promising,¹² these Ru complexes exhibit a major drawback. They are unable to penetrate cells membranes. Indeed, in the presence of viable cells, $[\text{Ru}(\text{bpy})_3]^{2+}$ (bpy = 2,2'-bipyridine) and $[\text{Ru}(\text{phen})_3]^{2+}$ (phen = 1,10-phenanthroline), which are structurally similar to

the above-mentioned complexes but do not photooxidize G units, tend to accumulate in internal vesicles. They are thus unable to reach the cytoplasm or nucleus where they should play their role of nucleic-acid-damaging agents.^{14,15} To use these complexes in phototherapy, methods for increasing their cellular uptake are needed. One possible strategy is presented in this work. We have chemically anchored DNA photoreactive Ru(II) complexes on biodegradable polymeric carriers that facilitate cellular membrane penetration. We have selected the polymer poly-[N-(2-hydroxyethyl)-L-glutamine] (PHEG) (Figure 1), which according to literature data is nontoxic and nonimmunogenic.¹⁶ Moreover, it can be easily derivatized, which allows subsequent coupling with drugs.^{17–21} It has also been demonstrated that this synthetic poly(amino acid) polymer is an excellent substrate for lysosomal enzymes;^{16,22} its digestion prevents accumulation of the polymer in the body. However, the enhanced permeability of the cancerous vasculature tissue and the absence of a good lymphatic system allow the polymer to accumulate in tumor regions²³ and to penetrate into cells by endocytosis. As a result, the tethering of photoreactive Ru(II) complexes to the polymer should favor the cellular penetration of these metallic compounds, and the lysosomal enzymes could release the active complexes inside the cells.

In this work, we have prepared and studied different Ru–PHEG conjugates. The chemically anchored complexes are derivatives of $[\text{Ru}(\text{TAP})_3]^{2+}$ and $[\text{Ru}(\text{TAP})_2\text{phen}]^{2+}$ bearing an oxyamine-functionalized phen or TAP ligand (Figure 2). These complexes have been chosen because, as explained above, their excited states are able to oxidize the G moieties of DNA by electron transfer, which leads to the formation of G photoadducts. Polymers of two different molecular weights have been prepared: one of 80 kDa and one of 6 kDa. The goal of the

* Authors to whom correspondence should be addressed. Phone: +32-(0)26503017 (A.K.-D.); +32(0)92644497 (E.S.). E-mail: akirsch@ulb.ac.be; Etienne.Schacht@UGent.be.

[†] Université Libre de Bruxelles.

[‡] University of Ghent.

[§] Université Joseph Fourier: Université Joseph Fourier-Grenoble.

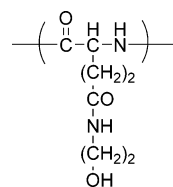


Figure 1. Structure of the PHEG polymer.

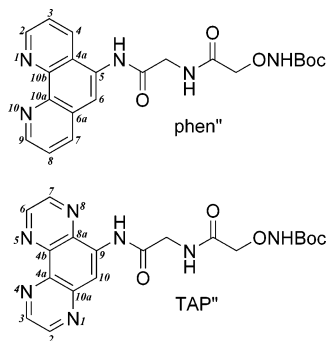


Figure 2. Structures of the two derivatized ligands phen'' and TAP''.

present work is to investigate whether the Ru complexes attached to these polymers keep their interesting properties versus the G units, even before digestion by lysosomal enzymes. Thus the behavior of these anchored complexes versus mono- and oligonucleotides containing G moieties has been examined.

Experimental Procedures

Syntheses. The methods of syntheses and purifications of the derivatized ligands phen''²⁴ and TAP''²⁵ have been published elsewhere. The complex Ru(TAP)₂Cl₂ has been synthesized according to the already described procedure.²⁶ [Ru(TAP)₂phen'']Cl₂ and [Ru(TAP)₂TAP'']Cl₂ have been prepared following the method reported in ref 25 via the intermediate [Ru(TAP)₂(H₂O)₂]²⁺. We report in this work the full attribution of the ¹H and ¹³C NMR spectra (see also Supporting Information for the spectra).

[Ru(TAP)₂phen'']Cl₂. ¹H NMR (300 MHz, *d*₆-DMSO) (for the numbering of the protons, see Figures 2 and 3) δ , ppm: 1.40 (s, 9H, *t*-Bu), 4.23 (d, *J* = 5.5 Hz, 2H, CH₂NH), 4.28 (s, 2H, CH₂O), 7.74 (dd, *J* = 8 Hz, *J* = 5 Hz, 1H, H^{P₈}), 7.82 (dd, *J* = 8 Hz, *J* = 5 Hz, 1H, H^{P₃}), 8.17 (d, *J* = 5 Hz, 1H, H^{P₉}), 8.23 (d and d, *J* = 3 Hz, 2H, H^{T_{3,3'}}), 8.30 (d, *J* = 5 Hz, 1H, H^{P₂}), 8.47 (m, 2H + NH, H^{T_{6,6'}} + CH₂NH), 8.62 (s, 1H, H^{P₆}), 8.65 (s, 4H, H^{T_{9,9'},10,10'), 8.79 (d, *J* = 8 Hz, H^{P₇}), 8.99 (d, *J* = 8 Hz, H^{P₄}), 9.04 (m, 4H, H^{T_{2,2'},7,7'), 10.32 (s, 1NH, phen-NH), 10.71 (s, 1NH, ONHBoc). ¹³C NMR (300 MHz, *d*₆-DMSO) δ , ppm: 27.87 (CH₃, *t*-Bu), 42.57 (CH₂NH), 74.54 (CH₂O), 80.47 (C, *t*-Bu), 119.37 (C^{P₆}-H), 125.60 (C^{P₃}-H), 126.42 (C^{P₈}-H), 130.20 (C^{P₅}), 132.30 (C^{T_{9,9'},10,10'-H), 133.53 (C^{P₄}-H), 136.95 (C^{P_{4a}}), 137.32 (C^{P₇}-H), 141.84 (C^{T_{4a,4a'},4b,4b'), 141.89 (C^{P_{6a}}), 144.13 (C^{P_{10a}}), 144.42 (C^{T_{8a,8a'},10a,10a'), 146.75 (C^{P_{10b}}), 148.58 (C^{T_{3,3'}}-H), 149.49 (C^{T_{6,6'}}-H), 149.59 (C^{T_{2,2'},7,7'-H), 152.76 (C^{P₉}-H), 153.98 (C^{P₂}-H), 156.60 (NH-CO-O), 168.57 and 168.96 (2 NH-CO-CH₂). ES-MS calcd for C₄₁H₃₅N₁₃O₅Ru, 890.88; found, 445.6 [M]²⁺, 962.2 [M]Cl⁺.}}}}}}

[Ru(TAP)₂TAP'']Cl₂. ¹H NMR (300 MHz, *d*₆-DMSO) (for the numbering of the protons, see Figures 2 and 3) δ , ppm: 1.41 (s, 9H, *t*-Bu), 4.29 (d, *J* = 6 Hz, 2H, CH₂NH), 4.30 (s, 2H, CH₂O), 8.35 (d, *J* = 3 Hz, 1H, H^{T₃}), 8.52 (m, 4H, H^{T_{3,3'},6,6'), 8.58 (d, *J* = 3 Hz, 1H, H^{T₆}), 8.67 (s, 4H, H^{T_{9,9'},10,10'), 8.72 (t, *J* = 6 Hz, 1NH, CH₂NH), 8.99 (d, *J* = 3 Hz, 1H, H^{T₂}), 9.04 (d, *J* = 3 Hz, 1H, H^{T₇}), 9.09 (m, 4H, H^{T_{2,2'},7,7'), 9.26 (s, 1H, H^{T₁₀}), 10.38 (s, 1NH, TAP-NH), 10.89 (s, 1NH, ONHBoc). ¹³C NMR (300 MHz, *d*₆-DMSO) δ , ppm: 27.86 (CH₃, *t*-Bu), 43.18 (CH₂NH), 74.39 (CH₂O), 80.50 (C, *t*-Bu), 115.39 (C^{T₁₀}-H), 132.18 (C^{T_{9,9'},10,10'-H), 137.08 (C^{T_{4a}}), 137.36 (C^{T_{4b}} or 8a), 137.96 (C^{T_{4b}} or 8a), 141.35 (C^{T_{4a,4a'},4b,4b'), 141.72 (C^{T_{10a}}), 144.38 (C^{T_{8a,8a'},10a,10a'),}}}}}}

145.22 (C^{T₉}), 147.43 (C^{T₃}-H), 147.86 (C^{T₇}-H), 149.67 (C^{T_{2,2'},3,3',6,6',7,7'-H), 150.20 (C^{T₂}-H or C^{T₆}-H), 150.23 (C^{T₂}-H or C^{T₆}-H), 156.61 (NH-CO-O), 168.84 and 169.33 (2 NH-CO-CH₂). ES-MS calcd for C₃₉H₃₃N₁₅O₅Ru, 892.86; found, 446.6 [M]²⁺, 928.2 [M]Cl⁺.}

Polymer. *N*-Carboxyanhydride of γ -benzyl-L-glutamate (NCA-BG) was prepared by its reaction with diphosgene in dry ethylacetate at 60 °C. The product is recrystallized from ethylacetate and dried under vacuum. The polymerization of NCA-BG was carried out in dry dichloromethane/ethyl acetate solution (5:1, v/v) at room temperature using 2-methoxyethylamine as the initiator for the low-molecular-weight polymer (9 kDa) and tributylamine for the high-molecular-weight polymer (121 kDa). The reaction was followed by IR spectroscopy. Poly(γ -benzyl-L-glutamate) was aminolyzed in *N,N*-dimethylformamide at room temperature with a mixture containing 10 mol % 3-amino-1,2-propanediol and 90 mol % 2-aminoethanol using 2-hydroxypyridine as a catalyst. The product obtained, PHEG with side vicinal diol groups, was precipitated in diethyl ether/ethanol (2:1, v/v), filtered, and dried under vacuum. The polymer was purified by preparative gel permeation chromatography (GPC; Sephadex G-25, water as an eluent) and lyophilized; its polydispersity from GPC analyses corresponds to about 1.5. The oxidation reaction of PHEG with NaIO₄ was performed in phosphate buffer pH 7.0 at room temperature, under argon, in darkness, for 3 h. The polymer obtained (PHEG-CHO) was purified using a PD10 desalting column, containing Sephadex G25, with 0.01 M phosphate buffer (pH 7.0) as the eluent.

Tethering of the Complexes to the Polymer. The oxyamine function of the complexes [Ru(TAP)₂TAP'']²⁺ and [Ru(TAP)₂phen'']²⁺ was deprotected from the Boc group in CH₂Cl₂/trifluoroacetic acid (TFA) (1:1, v/v) for 2 h. The solvent was removed by evaporation under vacuum, and the product was redissolved in 20 mM ammonium acetate buffer, pH 4.5. The solutions of PHEG-CHO and deprotected Ru(II) complex were mixed together. After 5 h of reaction, the product was purified using preparative GPC (Sephadex G25 with water as the eluent). The final conjugate was isolated by lyophilization. The high-performance liquid chromatography (HPLC) analysis at 408 nm showed that the products contain only Ru(II)-PHEG conjugates.

Materials. Tributylamine, 2-methoxyethylamine, *N,N*-dimethylformamide, 2-aminoethanol, 3-amino-1,2-propanediol, ethylacetate, diethyl ether, and dichloromethane were purified by distillation from calcium hydride under vacuum. 2-Hydroxypyridine, dichloroacetic acid, and trifluoroacetic acid were used as received.

The concentrations of the metal-containing conjugates were determined by optical absorption using the absorption coefficient ϵ of the complexes given in the literature.^{27,28} The Tris-HCl buffer (1 M, pH 7) stock solution was purchased from Sigma, and water was purified with a Millipore Milli-Q system. GMP was purchased from Sigma. The oligonucleotides were prepared by automated DNA synthesis on an Expedite DNA Synthesizer (Perkin-Elmer) using standard β -cyanoethylphosphoramidite chemistry on a 1 μ M scale. They were purified by reverse-phase HPLC and preparative polyacrylamide gel electrophoresis.

Instrumentation. The molecular weight of the poly(γ -benzyl-L-glutamate) was determined by viscosimetry in dichloroacetic acid. The molecular weight of PHEG was determined by analytical GPC using Hema Bio 40, 100, 300, and 1000 columns (Tessek, Prague, Czech Republic) with refractive index (RI) and multiangle laser light scattering (MALLS) detectors. The content of the vicinal diol groups in PHEG was determined by ¹H NMR (D₂O) spectroscopy. The Ru(II)-PHEG conjugates were analyzed by HPLC (Bio-Sil SEC-125 column (Bio Rad), citrate buffer (pH 6.0) as the eluent, UV-vis detector, λ = 408 nm).

The absorption and emission spectra and emission intensities and lifetimes were recorded at room temperature in buffer solutions (100 mM Tris-HCl, pH 7). When the measurements were carried out under argon, the solutions were deoxygenated with argon for at least 45 min before and during all experiments. The absorption spectra were recorded on a Perkin-Elmer Lambda UV-vis spectrophotometer. All of the emission spectra were recorded on a Shimadzu RF-5001 PC spectro-

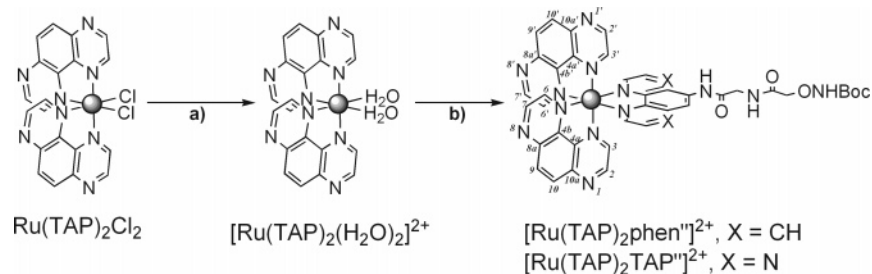


Figure 3. Preparation of the $[\text{Ru(TAP)}_2\text{phen}'']^{2+}$ and $[\text{Ru(TAP)}_2\text{TAP}'']^{2+}$ complexes. Reagents and conditions: (a) AgNO_3 , H_2O , 2 h, 100 °C; (b) phen'' or TAP'', DMF, 1 h, 100 °C, Ar.

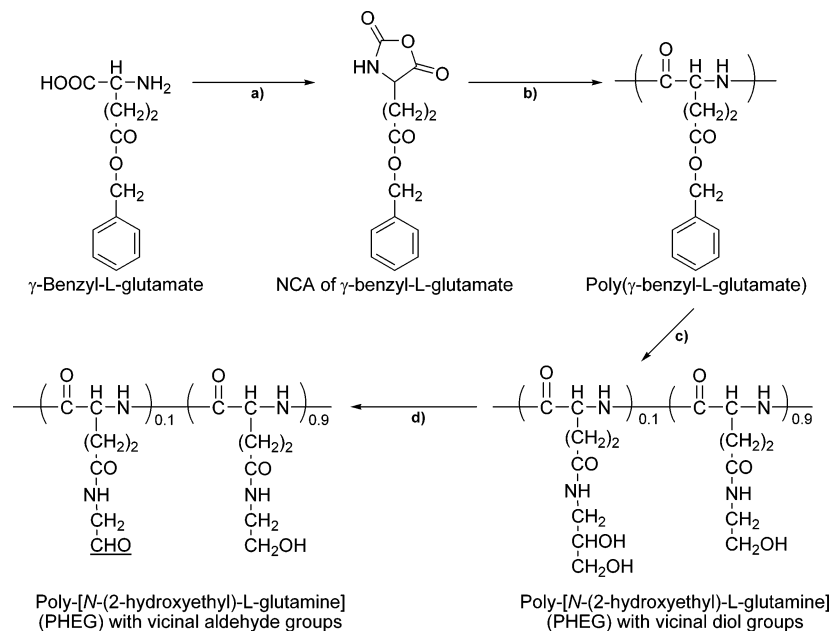


Figure 4. Synthesis of PHEG with vicinal aldehyde groups. Reagents and conditions: (a) $(\text{COCl}_2)_2$, AcOEt , 60 °C; (b) polymerization with 2-methoxyethylamine or tributylamine, $\text{CH}_2\text{Cl}_2/\text{AcOEt}$ (5:1, v/v), room temperature; (c) 3-amino-1,2-propanediol (10 mol %) and 2-aminoethanol (90 mol %), DMF, 2-hydroxypyridine, room temperature; (d) NaIO_4 , phosphate buffer (pH 7.0), room temperature.

fluorimeter equipped with a xenon lamp (250 W) as the excitation source and a Hamamatsu R-298 red-sensitive photomultiplier tube for detection. The spectra were corrected for the instrument response. The luminescence lifetime measurements were performed with a time-resolved single-photon counting (SPC), Edinburgh Instruments (Edinburgh, U. K.) FL-900 spectrophotometer, equipped with a nitrogen-filled discharge lamp and a Peltier cooled Hamamatsu R-995 photomultiplier tube. The emission decays were analyzed with the Edinburgh Instruments software (version 3.00), based on nonlinear least-squares regressions using a modified Marquardt algorithm. Excitation at 379 nm was used, and the emission was measured at the emission maximum for each complex.

Steady-State Irradiation in the Presence of GMP. Steady-state illuminations were performed with a mercury vapor lamp (Osram HBO, 200 W) and a quartz halogen lamp (Philips, 2000 W), cooled by a system of water circulation. IR (water) and UV (KNO_3) cutoff filters were inserted between the irradiation cell and the exciting sources. All experiments were performed with argon-saturated solutions (2 mL) containing $\text{Ru(II)}\text{-PHEG}$ conjugates (10^{-5} M, expressed in Ru(II) complex concentration) and GMP (10^{-3} M) in buffered solutions (100 mM Tris-HCl, pH 7).

Gel Electrophoresis. The oligonucleotides were 5'-end-labeled by T4 polynucleotide kinase using 3000 Ci mmol^{-1} [$\gamma\text{-}^{32}\text{P}$]-ATP (Amersham) at 37 °C for 30 min. The addition of 5 μL of a 10 wt % EDTA aqueous solution stops the kinase activity. Excess ATP and kinase were removed by exclusion chromatography with Micro Bio-Spin P-6 in Tris buffer (Bio-Rad). A solution of the complex conjugates (15 μM) in 5 mM Tris-HCl buffer (pH 7) and ^{32}P -labeled single-stranded oligonucleotides (55 μM in base) was illuminated for 15 and 30 min at 442 nm

at room temperature with a monochromatic laser (He-Cd, Melles Griot, 35 mW). To the samples of the different mixtures (10 μL), the loading buffer (89 mM Tris-HCl, pH 8, 89 mM boric acid, 2 mM EDTA, 7 M urea, 12% Ficoll, 0.02% xylene cyanol, 0.01% bromophenol) (10 μL) was added. The DNA species were separated by electrophoresis on a polyacrylamide gel (10% with a ratio of 19:1 of acrylamide to bisacrylamide) containing urea (7 M) in TBE buffer (90 mM Tris-borate, pH 8, 2 mM EDTA). The different DNA fragments were visualized by autoradiography with Phosphor Screen and were counted with a phosphorimager (Storm 860 instrument).

Results

Syntheses of the Conjugates. Derivatized Ligands and Corresponding Complexes. The TAP ligand derivatized with the oxyamine function (Figure 2) was prepared²⁵ according to the procedure described for the phen'' derivative.²⁴ The synthesis consists of the following main steps. Starting from 9-amino-TAP,²⁹ the glycine linker was introduced by reaction with the corresponding anhydride of *N*-(*tert*-butoxycarbonyl)glycine. The *tert*-butoxycarbonyl group was removed by acidic treatment in $\text{CH}_2\text{Cl}_2/\text{TFA}$ (50:50, v/v). Introduction of the oxyamino group was achieved by coupling the activated ester of *N*-Boc-*O*-(carboxymethyl)-hydroxylamine³⁰ with the amino derivative obtained in the previous step. The protected oxyamino derivative was purified by column chromatography as a white powder (45% overall yield from the 9-amino-TAP).

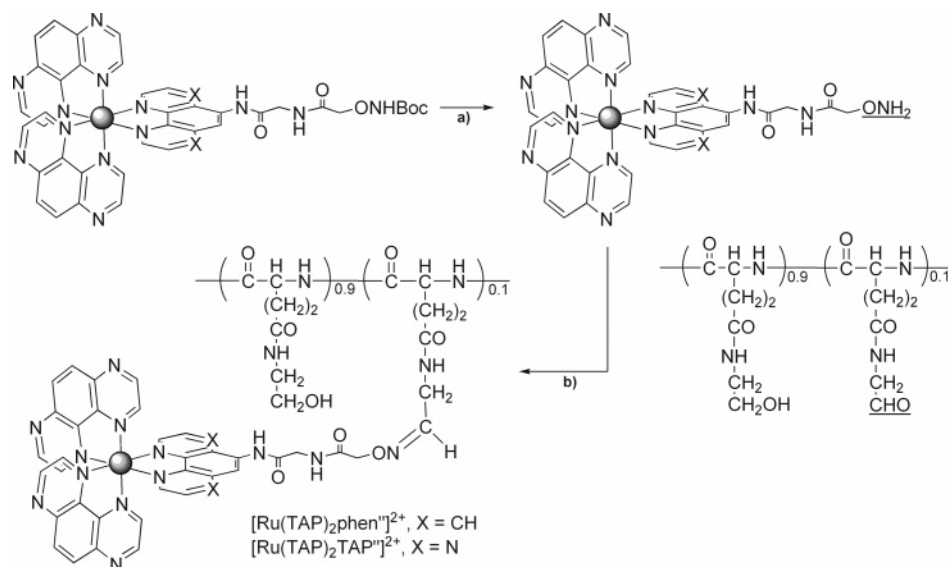


Figure 5. Synthesis of Ru(II) complex-PHEG conjugates. Reagents and conditions: (a) $\text{CH}_2\text{Cl}_2/\text{TFA}$ (1:1, v/v); (b) ammonium acetate buffer (pH 4.5).

The complexes $[\text{Ru}(\text{TAP})_2\text{phen}']\text{Cl}_2$ and $[\text{Ru}(\text{TAP})_2\text{TAP}']\text{Cl}_2$ were obtained by the straightforward synthesis illustrated in Figure 3. The precursor $\text{Ru}(\text{TAP})_2\text{Cl}_2$ was synthesized from RuCl_3 and TAP ligand as already described.²⁶ After activation of the precursor $\text{Ru}(\text{TAP})_2\text{Cl}_2$ into $[\text{Ru}(\text{TAP})_2(\text{H}_2\text{O})_2]^{2+}$ according to previously described conditions,³¹ the complexes were obtained after substitution of the two water molecules by the protected oxyamino phenanthroline or tetraazaphenanthrene in dimethylformamide (DMF); they were purified by column chromatography with a 70% overall yield.

PHEG with Vicinal Aldehyde Groups. The precursor for PHEG, i.e., poly(γ -benzyl-L-glutamate), was prepared by polymerization of NCA-BG using 2-methoxyethylamine as an initiator for the low-molecular-weight polymer (9 kDa) and tributylamine for the high-molecular-weight polymer (121 kDa) (Figure 4). After aminolysis of poly(γ -benzyl-L-glutamate) with a mixture of 3-amino-1,2-propanediol (10 mol %) and 2-aminoethanol (90 mol %), the (PHEG polymers with molecular weights of 6 and 80 kDa, respectively, and containing side vicinal diol groups were obtained. Finally, PHEG was oxidized with NaIO_4 to prepare the polymers with aldehyde groups.

Coupling of the Ru(II) Complex to the PHEG Polymer. After deprotection of the oxyamine function of the two complexes in acidic conditions, the Ru(II)-PHEG conjugates were obtained by coupling of the deprotected Ru(II) complexes via an oxime ether linkage to PHEG-containing pendent aldehyde groups (Figure 5). The percentage of labeling by the Ru(II) complex in the conjugate, determined by UV-vis spectroscopy at 408 nm, is 7.0 wt % (2.3 mol %) in RuT_3 -PHEG (80 kDa), 6.0 wt % (2.0 mol %) in RuT_3 -PHEG (6 kDa), and 6.3 wt % (2.1 mol %) in RuT_2P -PHEG (6 kDa) (mol % is determined as the percentage of ruthenium(II) complex per 100 monomer units in the polymer).

Absorption, Luminescence, and Photostability of the Ru(II)-PHEG Conjugates. The spectroscopic absorption and emission data recorded for the Ru(II)-PHEG conjugates are gathered in Table 1 along with those of the free complexes $[\text{Ru}(\text{TAP})_2\text{TAP}']^{2+}$ and $[\text{Ru}(\text{TAP})_2\text{phen}']^{2+}$ for comparison purposes. The absorption and emission spectra are displayed in Figures 6 and S2, respectively. The Ru(II)-polymer conjugates show the characteristic metal-to-ligand charge transfer (MLCT) and ligand-centered (LC) bands of the free Ru(II) complexes

Table 1. Spectroscopic Data for the Ru(II) Complex-Polymer Conjugates^a

sample	absorption		excited-state	
	λ_{max} (nm)		λ_{max} (nm)	lifetime ^c τ (ns)
RuT_3 -PHEG (80 kDa)	406	277	602	236
RuT_3 -PHEG (6 kDa)	406	279	604	219
RuT_2P -PHEG (6 kDa)	414	273	646	709
$[\text{Ru}(\text{TAP})_2\text{TAP}']^{2+}$	406	278	601	226
$[\text{Ru}(\text{TAP})_2\text{phen}']^{2+}$	414	273	645	724

^a All of the measurements were performed at room temperature in air-saturated buffer solutions (100 mM Tris-HCl, pH 7). ^b Excitation at the maximum of visible absorption, 406 nm, for the $[\text{Ru}(\text{TAP})_2\text{TAP}']^{2+}$ conjugate and 414 nm for the $[\text{Ru}(\text{TAP})_2\text{phen}']^{2+}$ conjugate. ^c Emission monitored at the wavelength of the maximum ($\lambda_{\text{exc}} = 379$ nm); the luminescence decays analyzed according to a monoexponential function: $I_{\text{em}} = A \exp(-t/\tau)$, estimated error for $\tau \approx 3\%$.

at 400–450 and 250–320 nm, respectively. An important increase of the absorption is observed below 240 nm, which is due to the polymer absorption. However, the Ru(II)-PHEG conjugates show structureless emission at room temperature. This emission is typical of Ru(II) polypyridyl complexes and originates from the ³MLCT excited state involving a TAP ligand for both metallic compounds. The emission intensities, for the same percentage of absorbed light, are very similar for the free and the polymer-anchored complexes. Time-resolved luminescence analyses under pulsed illumination lead to single-exponential decays with corresponding excited-state lifetimes (Table 1) close to the values determined for the free complexes (less than 2% difference).

The stabilities of the Ru(II)-PHEG conjugates under steady-state illumination also have been tested. It was shown previously that the free complex $[\text{Ru}(\text{TAP})_3]^{2+}$ gives rise to the loss of a ligand under illumination at pH 7. This is demonstrated by a decrease of the 400 nm absorption band and the appearance of a new absorption at 500 nm due to the formation of $[\text{Ru}(\text{II})-(\text{TAP})_2\text{XY}]^{n+}$ (X and Y are H_2O , Cl^-) corresponding to photo-dechelated products.²⁷ This photoreaction is not observed with $[\text{Ru}(\text{TAP})_2\text{phen}]^{2+}$, which does not cross as easily as the tris-homoleptic complex $[\text{Ru}(\text{TAP})_3]^{2+}$ to the triplet metal-centered state (³MC) responsible for the dechelation. To check whether the attachment to the polymer could influence the behavior of these two metallic compounds, the UV-vis absorption of the

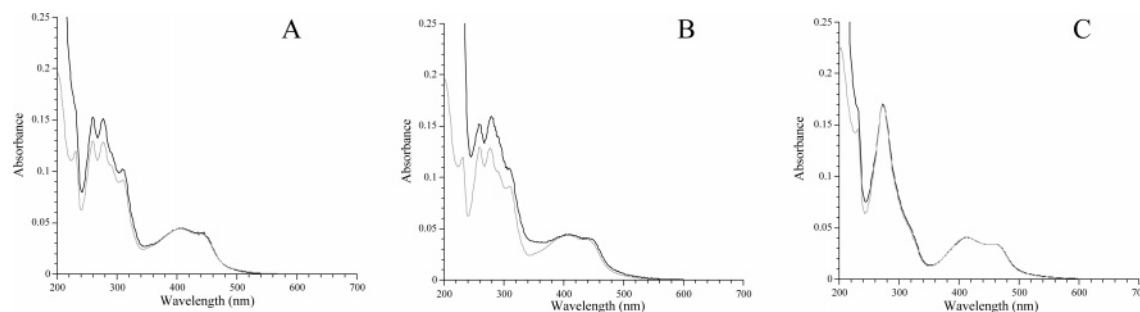


Figure 6. Absorption spectra of (A) the complex $[\text{Ru}(\text{TAP})_2\text{TAP}']^{2+}$ (gray line) and the conjugate $\text{RuT}_3\text{-PHEG}$ (80 kDa) (dark line), (B) the complex $[\text{Ru}(\text{TAP})_2\text{TAP}']^{2+}$ (gray line) and the conjugate $\text{RuT}_3\text{-PHEG}$ (6 kDa) (dark line), and (C) the complex $[\text{Ru}(\text{TAP})_2\text{phen}']^{2+}$ (gray line) and the conjugate $\text{RuT}_2\text{P-PHEG}$ (6 kDa) (dark line). Measurements were performed in aqueous buffered solutions (100 mM Tris-HCl, pH 7); the absorbance was adjusted at 0.04 at the maximum of absorbance of the MLCT band in the three cases.

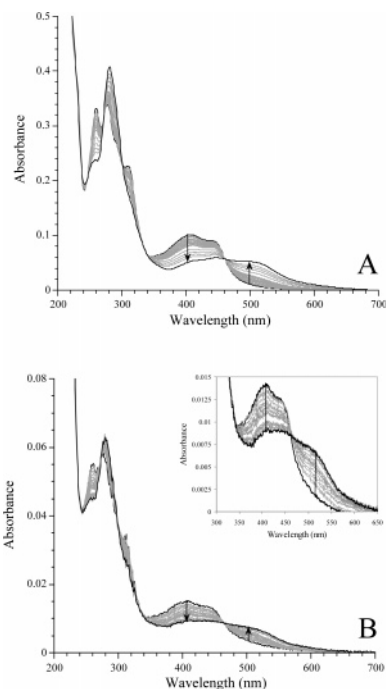


Figure 7. Absorption spectra for (A) $\text{RuT}_3\text{-PHEG}$ (80 kDa) and (B) $\text{RuT}_3\text{-PHEG}$ (6 kDa) after visible light irradiation (from 0 until 60 min). The inset in part B illustrates the changes in the MLCT band. The measurements were recorded in aqueous buffer (100 mM Tris-HCl, pH 7).

Ru-PHEG conjugates has been monitored during steady-state illumination. Figure 7 shows the absorption spectra obtained after 1 h of illumination of the $\text{RuT}_3\text{-PHEG}$ (80 kDa) and $\text{RuT}_3\text{-PHEG}$ (6 kDa) conjugates in buffered solution (100 mM Tris-HCl, pH 7). In both cases, there is a decrease of the 400 nm absorption band and the appearance of a new one at 500 nm as for the nontethered complex. For the $\text{RuT}_2\text{P-PHEG}$ (6 kDa) conjugate no spectral changes are detected in the same conditions (data not shown).

Photochemical Behavior of the Ru(II)-PHEG Conjugates with G Moieties. *With GMP.* Luminescence quenching experiments of the Ru(II)-PHEG conjugates by GMP were carried out at room temperature in air-saturated solutions at pH 7 (100 mM Tris-HCl buffer). All of the plots are linear, and the corresponding quenching rate constants for the three conjugates are collected in Table 2 along with the values obtained for the corresponding free complexes. These data indicate that the quenching rate constants for the Ru(II) complexes anchored to the polymer are slightly lower than those for the free complexes.

Previous studies of the free TAP complexes in the presence of G units showed that the intermediate species formed after

Table 2. Quenching Rate Constants by GMP, Determined from the Linear Stern-Volmer Plots in Emission Intensity (100 mM Tris-HCl Buffer, pH 7)

sample	k_q ($\text{M}^{-1}\text{s}^{-1}$)
$\text{RuT}_3\text{-PHEG}$ (80 kDa)	1.5×10^9
$\text{RuT}_3\text{-PHEG}$ (6 kDa)	1.4×10^9
$\text{RuT}_2\text{P-PHEG}$ (6 kDa)	0.54×10^9
$[\text{Ru}(\text{TAP})_3]^{2+}$ 11	2.2×10^9
$[\text{Ru}(\text{TAP})_2\text{phen}]^{2+}$ 11	0.98×10^9

the photoelectron transfer led to a photoadduct of the G moiety on one of the TAP ligands of the complex. Formation of this photoproduct can be easily followed by the appearance under illumination, of a hyperchromic effect around 350–450 nm in the Ru(II) complex absorption spectrum.³²

Figure 8 shows the modifications in the absorption spectra of the three conjugates under illumination in the presence of GMP in deoxygenated solution. A hyperchromic effect around 350–420 nm is demonstrated for the $\text{RuT}_2\text{P-PHEG}$ (6 kDa) conjugate, which can be attributed to the formation of a photoadduct. This increase is indeed similar to that observed for the free complex.³² With the $\text{RuT}_3\text{-PHEG}$ conjugates (6 and 80 kDa) the light-induced changes are more complicated because of the presence of a photo-dechelation process (Figures 8A and 8B). Indeed, in addition to the hyperchromic effect at 350 nm due to photoadduct formation, an absorption increase due to photo-dechelation appears clearly at 500 nm.

With Oligonucleotides. Photoadduct formation also can be detected with an oligonucleotide containing G moieties, and such a photoreaction can be easily followed by polyacrylamide gel electrophoresis experiments in denaturing conditions.³³ In these series of experiments a ^{32}P -5'-end-labeled single-stranded oligonucleotide containing two guanine units in its sequence (3'-AGG AAA ATA ATT TAA AT-5') was irradiated with a 442 nm light source in the presence of the two small conjugates, $\text{RuT}_3\text{-PHEG}$ (6 kDa) and $\text{RuT}_2\text{P-PHEG}$ (6 kDa), successively. To compare the results, the illuminations with the same ODN in the presence of the free $[\text{Ru}(\text{TAP})_2\text{phen}']^{2+}$ and $[\text{Ru}(\text{TAP})_2\text{TAP}']^{2+}$ complexes were also performed. Figure 9 shows the results of a typical electrophoresis experiment carried out with a sample of the conjugates or the free complexes illuminated in an aerated 5 mM Tris-HCl (pH 7) buffered solution containing the 17-mer ^{32}P -labeled oligonucleotides.

Lanes A, D, G, and J correspond to the samples before illumination. The only spot observed in this case corresponds to the 17-mer oligonucleotide. Lanes C, F, I, and L show the effects of a 30 min illumination in the presence of the conjugates or the free complexes. For the free complexes, one or two

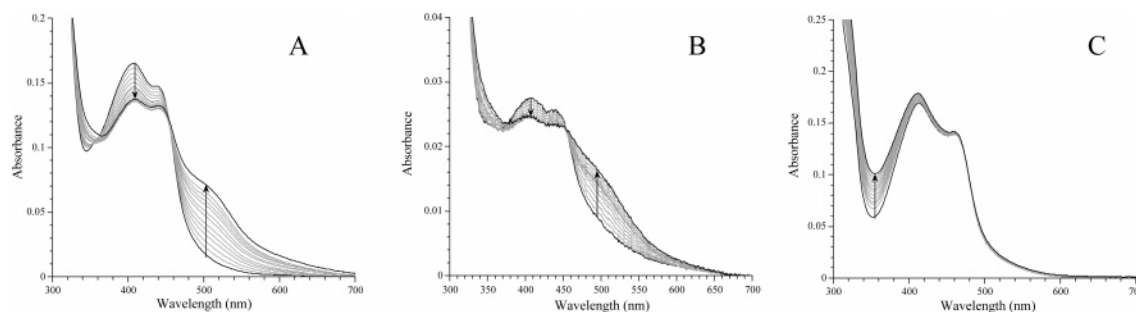


Figure 8. Absorption spectra of (A) RuT₃-PHEG (80 kDa), (B) RuT₃-PHEG (6 kDa), and (C) RuT₂P-PHEG (6 kDa) as a function of visible irradiation, from 0 until 60 min, in the presence of GMP (10⁻³M) under argon, in aqueous buffer solution (100 mM Tris-HCl, pH 7).

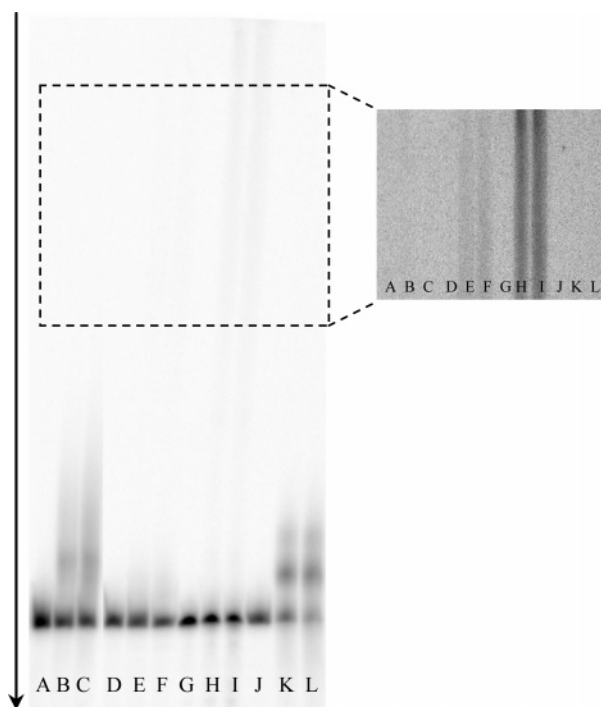


Figure 9. Autoradiogram of a 10% denaturing polyacrylamide gel showing the ³²P-end-labeled 17-mer in the presence of RuT₃-PHEG (6 kDa), RuT₂P-PHEG (6 kDa), [Ru(TAP)₂TAP']²⁺, and [Ru(TAP)₂phen']²⁺. Lanes A–C: illumination of [Ru(TAP)₂TAP']²⁺ for 0, 15, and 30 min. Lanes D–F: illumination of RuT₃-PHEG (6 kDa) for 0, 15, and 30 min. Lanes G–I: illumination of RuT₂P-PHEG (6 kDa) for 0, 15, and 30 min. Lanes J–L: illumination of [Ru(TAP)₂phen']²⁺ for 0, 15, and 30 min. The inset shows the smears by increasing the time of radioactivity counting. The reaction mixture contained 1 pmol of 5'-³²P-labeled single-stranded oligonucleotide, 5 mM Tris-HCl, pH 7 in a total volume of 10 μ L.

delayed spots appear; they correspond to the formation of one or two adducts of the free complexes on the two accessible G units of the oligonucleotide. In contrast, for the two PHEG 6 kDa conjugates, the illumination does not lead to these spots but to the appearance of a smear of radioactivity (lanes E, F, H, and I) on the gel due to species with different lower mobilities. Incubation of the oligonucleotide in the presence of the conjugates in the dark does not produce these retarded smears. The quantification of the radioactivity of the smears results in 2% and 8% photoadduct after 30 min of illumination for RuT₃-PHEG (6 kDa) and RuT₂P-PHEG (6 kDa), respectively (Table 3) and in 45% and 75% photoadduct formation for the free [Ru(TAP)₂TAP']²⁺ and [Ru(TAP)₂phen']²⁺, respectively.

When the same procedure is applied to the large conjugate RuT₃-PHEG (80 kDa), only traces (<2%) of radioactivity are detected in the wells of the gel due to the very low mobility

Table 3. Percentages of Photoadduct Formation^a

sample	photoadduct formation (%)
RuT ₃ -PHEG (6 kDa)	2
RuT ₂ P-PHEG (6 kDa)	8
[Ru(TAP) ₂ TAP'] ²⁺	45
[Ru(TAP) ₂ phen'] ²⁺	75

^a Yields are given for 30 min of continuous illumination of a solution containing 5'-³²P-labeled single-stranded oligonucleotides. The intensity of the smear corresponding to the photoadduct was compared to the total radioactivity measured in each lane.

species unable to migrate through the gel; they could be attributed to the formation of the photoadduct between the complex anchored to the PHEG and the guanine units of the single-stranded oligonucleotide. Even when the percentage of acrylamide in the gel was reduced from 10% to 5%, the radioactivity for this species was still concentrated in the wells, and no quantification was possible.

Discussion

Three different conjugates have been prepared with polymers of two different lengths (6 and 80 kDa), chemically derivatized by two different complexes photoreactive with guanine moieties. The shorter 6kDa polymer, once inside the cells, should be digested relatively rapidly by enzymes that would liberate the photoactive drug. The higher-molecular-weight 80kDa polymer should be degraded less easily. Therefore, it is essential to test in that case whether the metal complex is still photoreactive versus DNA while attached to the polymer.^{34–36} Indeed in both cases, after or even before the complete digestion of the polymer, the complex could photodamage the nucleic acids. The two chemically tethered ruthenium(II) complexes present similar sizes and shapes; they have, however, a slightly different oxidation power in their ³MLCT state (reduction potentials of the excited states, $E_{\text{red}}^*([\text{Ru}(\text{TAP})_3]^{2+}) = +1.30$ V vs SCE and $E_{\text{red}}^*([\text{Ru}(\text{TAP})_2\text{phen}]^{2+}) = +1.15$ V vs SCE),³ and they exhibit a different photostability under continuous illumination in the absence of reactant. [Ru(TAP)₂phen]²⁺ is photostable whereas [Ru(TAP)₃]²⁺ undergoes photo-dechelation.³⁷ Therefore both complexes were tested; [Ru(TAP)₂phen]²⁺ was anchored on the small polymer, and [Ru(TAP)₃]²⁺ was anchored on the shorter and longer polymers to check, in addition to its photochemical behavior with G residues, whether the length of the polymer would influence the photo-dechelation process.

The photophysical properties of the three conjugates are very close to those of the respective free Ru(II) complexes. No shifts in the absorption or emission maxima are observed, which indicates that the microenvironment of the polymer around the complex has no influence on the electronic transitions. In

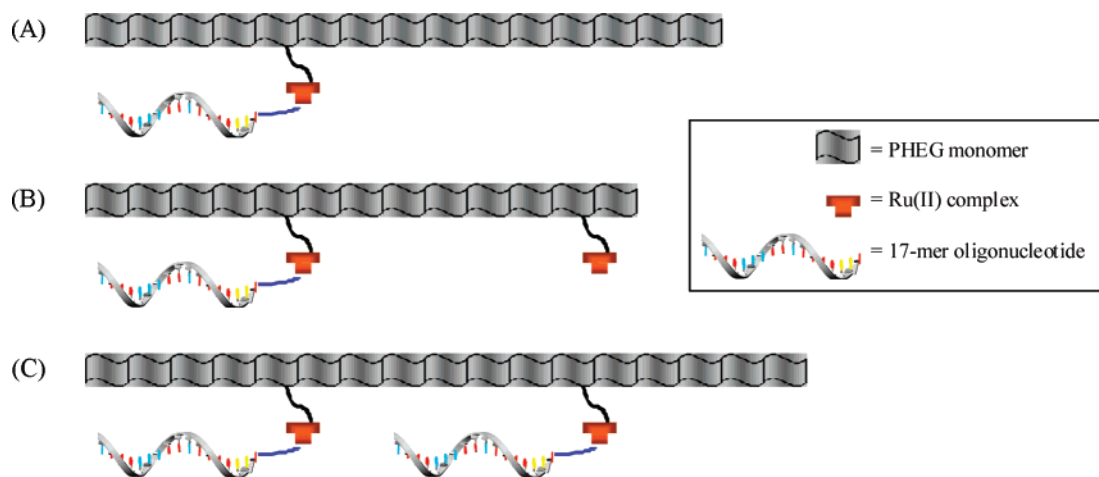


Figure 10. Schematic representation of possible components in the smear of radioactivity detected on the 10% acrylamide gel in denaturing conditions. (A) Polymer with one anchored complex that has photoreacted with an oligonucleotide. (B and C) Polymers with two anchored complexes where, respectively, only one or both have photoreacted with an oligonucleotide.

agreement with this, no significant differences in emission intensities or emission lifetimes are demonstrated between the linked and the free complexes. There are thus no changes in the rate constants of deactivation ($\tau^{-1} = k_r + k_{nr} + k_{MC} e^{-\Delta E/RT}$) of the excited state. Also, in agreement with these conclusions, the single-exponential emission decays under pulsed excitation mean that the excited complexes do not probe different microenvironments; they are not protected nor quenched by the polymer chain. These results concerning the photophysical behaviors are thus positive, considering future possible applications of these polymers.

Ru(II) complexes containing π -deficient ligands, such as those examined in this work, are strongly oxidizing in their $^3\text{MLCT}$ excited state with the oxidizing power increasing with the number of π -deficient ligands (number of TAP). Their emission is quenched by the reducing agent GMP, and the rate constant depends on the E_{red}^* value. Even when the complexes are tethered to the higher-molecular-weight polymers, their luminescence is quenched by GMP due to a photoinduced electron transfer from the guanine moiety of GMP to the excited complexes.^{11,38} The values of the quenching rate constants determined from Stern–Volmer plots (Table 2) are close to those found for the quenching of the excited states of the free complexes. This indicates again that the presence of the polymer attached to the complexes does not perturb their behavior because the electron transfer from GMP to the excited state is still very efficient. No significant difference could be demonstrated for the RuT_3 –PHEG (80 kDa) and RuT_3 –PHEG (6 kDa) conjugates. Thus increasing the length of the polymer chain does not prevent the photoinduced electron transfer from taking place. The studies under continuous illumination of the RuT_2P –PHEG (6 kDa) conjugate demonstrate the appearance of the characteristic hyperchromic effect around 350–420 nm attributed to the formation of a photoadduct “complex–GMP”. Nevertheless for the two $[\text{Ru}(\text{TAP})_3]^{2+}$ conjugates, the hyperchromic effect is not as clear because for these conjugates the photoadduct formation is in competition with the photo-dechelation process.

The photoadduct formation of the polymer conjugates on guanine residues is also demonstrated by gel electrophoresis experiments with a 17-mer oligonucleotide containing two G residues. In such a case, the photoreaction can be called photo-cross-linking between the ODN and the polymer. Thus, when the lower-molecular-weight conjugates are illuminated in the presence of a ^{32}P -labeled oligonucleotide, a smear of radioactivity corresponding to much lower mobility species is

observed. Incubation of the same oligonucleotide in the presence of the Ru(II)–PHEG conjugates in the dark does not produce these retarded bands or smear, which confirms that the covalent binding of the metal complexes to the oligonucleotides takes place under the action of light. Moreover, comparison with the photoadduct formation of the same oligonucleotide with the free complexes indicates that one or two photoadducts are detected with the free complex, whereas with the PHEG conjugates no spots are detected but only smears. These smears of radioactivity can therefore be attributed to the migration of photoadducts between the oligonucleotides and the Ru(II) complexes anchored to the PHEG polymers. (see Figure 10 for a schematic representation). Calculations lead to the conclusion that on average one complex is tethered to one 6 kDa polymer (11 complexes for 80 kDa polymers). The smears can thus originate from different factors. First, a polydispersity of the polymer of 1.5 leads to variable migrations of the different chain lengths, most probably with one but also with two complexes. Moreover, as also observed in previous works for the photo-cross-linkings between oligonucleotides,³³ depending on the position of the complex on the polymer (in the middle or at the end of the chain), the photo-cross-linkings will also generate compounds that exhibit different rates of migration on the gel.

A comparison of the percentage of radioactivity (Table 3) corresponding to the photoadduct formation with the free complexes and with the PHEG conjugates indicates that the formation of adducts, in the same conditions of illumination and concentration in the complex, is much lower for complexes tethered to the polymer. This drop of yield could be due to some steric hindrance between the polymer chain and the oligonucleotide that prevents the attached Ru(II) compound from adopting the correct geometry in the encounter species “Ru–guanine” for the formation of the photoadduct. However, the presence of some polymer remaining in the wells of the gel could be responsible for an underestimation of the photo-cross-linking yield. However, the lower percentage of photoadduct formation observed for RuT_3 –PHEG (6 kDa) in comparison to that for RuT_2P –PHEG (6 kDa) (Table 3) can be attributed to competition between the photo-dechelation process and photoadduct formation for RuT_3 –PHEG (6 kDa).

Conclusion

In this work, we have investigated the effect of the chemical anchoring of biodegradable polymers to photooxidizing Ru(II)

complexes. By comparing the photophysical properties of these attached metallic compounds to those of the free complexes and by examining their photochemical behaviors in the presence of two different sources of the guanine moiety, we have demonstrated that the Ru(II) complexes keep their interesting photoreactive properties toward the guanine moieties despite their attachment to high-molecular-weight polymers. Moreover, we have demonstrated by gel electrophoresis that these Ru-polymers are even capable, under illumination, to lead to the formation of a photoadduct with guanine-containing oligonucleotides. Because the presence of the polymer does not prevent the photodamage of the oligonucleotides by the photooxidizing complexes, the uptake of these Ru conjugates by the cells will be investigated in the future.

Acknowledgment. The authors thank the ARC program 2002–2007 (Action de Recherche Concertée) and the “Laboratoire Européen Associé” (LEA) between the FNRS (Fonds National pour la Recherche Scientifique, Belgium) and the CNRS (Centre National pour la Recherche Scientifique, France) for financial support. They are also grateful to the COST D35 and the Pôle d’Attraction Interuniversitaire (PAI, Belgium). S. D. thanks the Fonds pour la Recherche dans l’Industrie et l’Agriculture (FRIA) for a fellowship.

Supporting Information Available. ^1H NMR spectra of the two derivatized ruthenium(II) complexes and emission spectra of the ruthenium(II) complex–PHEG polymer conjugates. This material is available free of charge via the Internet at <http://pubs.acs.org>.

References and Notes

- Núñez, M. E.; Barton, J. K. *Curr. Opin. Chem. Biol.* **2000**, *4*, 199–206.
- Zhang, C. X.; Lippard, S. J. *Curr. Opin. Chem. Biol.* **2003**, *7*, 481–489.
- Elias, B.; Kirsch-De Mesmaeker, A. *Coord. Chem. Rev.* **2006**, *250*, 1627–1641.
- Clarke, M. J. *Coord. Chem. Rev.* **2003**, *236*, 209–233.
- Moucheron, C.; Kirsch-De Mesmaeker, A.; Kelly, J. M. In *Less Common Metals in Proteins and Nucleic Acid Probes*; Structure and Bonding 92; Springer-Verlag: Berlin, 1998; pp 164–216.
- Kelly, J. M.; Feeney, M. M.; Jacquet, L.; Kirsch-De Mesmaeker, A.; Lecomte, J.-P. *Pure Appl. Chem.* **1997**, *69*, 767–772.
- Blasius, R.; Nierengarten, H.; Luhmer, M.; Constant, J.-F.; Defrancq, E.; Dumy, P.; van Dorsselaer, A.; Moucheron, C.; Kirsch-De Mesmaeker, A. *Chem.—Eur. J.* **2005**, *11*, 1507–1517.
- Uji-i, H.; Foubert, P.; De Schryver, F.; De Feyter, S.; Gicquel, E.; Etoc, A.; Moucheron, C.; Kirsch-De Mesmaeker, A. *Chem.—Eur. J.* **2006**, *12*, 758–762.
- Jacquet, L.; Kelly, J. M.; Kirsch-De Mesmaeker, A. *Chem. Commun.* **1995**, 913–914.
- Jacquet, L.; Davies, D. R.; Kirsch-De Mesmaeker, A.; Kelly, J. M. *J. Am. Chem. Soc.* **1997**, *119*, 11763–11768.
- Lecomte, J.-P.; Kirsch-De Mesmaeker, A.; Feeney, M. M.; Kelly, J. M. *Inorg. Chem.* **1995**, *34*, 6481–6491.
- Pauly, M.; Kayser, I.; Schmitz, M.; Dicato, M.; Del Guerzo, A.; Kolber, I.; Moucheron, C.; Kirsch-De Mesmaeker, A. *Chem. Commun.* **2002**, 1086.
- Boerner, L. J. K.; Zaleski, J. M. *Curr. Opin. Chem. Biol.* **2005**, *9*, 135–144.
- Dobrucki, J. W. *J. Photochem. Photobiol., B* **2001**, *65*, 136–144.
- Jiménez-Hernandez, M. E.; Orellana, G.; Montero, F.; Portolés, M. T. *Photochem. Photobiol.* **2000**, *72*, 28–34.
- Pytela, J.; Saudek, V.; Drobnik, J.; Rypacek, F. *J. Controlled Release* **1989**, *10*, 17–25.
- De Marre, A.; Schacht, E. *Makromol. Chem.* **1992**, *193*, 3023–3030.
- De Marre, A.; Soye, H.; Schacht, E.; Shoaibi, M. A.; Seymour, L. W.; Rihova, B. *J. Controlled Release* **1995**, *36*, 87–97.
- Soyez, H.; Schacht, E. *J. Controlled Release* **1997**, *45*, 235–247.
- Soyez, H.; Seymour, L. W.; Schacht, E. *J. Controlled Release* **1999**, *57*, 187–196.
- Hoste, K.; Schacht, E.; Seymour, L. W. *J. Controlled Release* **2000**, *64*, 53–61.
- Hayashi, T.; Nakanishi, E.; Iizuka, Y.; Oya, M.; Iwatsuki, M. *Eur. Polym. J.* **1995**, *31*, 453–458.
- Maeda, H.; Seymour, L. W.; Miyamoto, Y. *Bioconjugate Chem.* **1992**, *3*, 351–362.
- Deroo, S.; Defrancq, E.; Moucheron, C.; Kirsch-De Mesmaeker, A.; Dumy, P. *Tetrahedron Lett.* **2003**, *44*, 8379–8382.
- Villien, M.; Deroo, S.; Gicquel, E.; Defrancq, E.; Moucheron, C.; Kirsch-De Mesmaeker, A.; Dumy, P. *Tetrahedron* **2007**, *63*, 11299–11306.
- Kirsch-De Mesmaeker, A.; Jacquet, L.; Nasielski, J. *Inorg. Chem.* **1988**, *27*, 4451–4458.
- Lecomte, J.-P.; Kirsch-De Mesmaeker, A.; Kelly, J. M. *Bull. Soc. Chim. Belg.* **1994**, *103*, 193–200.
- Ortmans, I.; Elias, B.; Kelly, J. M.; Moucheron, C.; Kirsch-De Mesmaeker, A. *Dalton Trans.* **2004**, 668–676.
- Nasielski-Hinkens, R.; Benedek-Vamos, M.; Maetens, D. *J. Heterocycl. Chem.* **1980**, *17*, 873–876.
- Ide, H.; Akamatsu, K.; Kimura, Y.; Michiue, K.; Makino, K.; Asaeda, A.; Takamori, Y.; Kubo, K. *Biochemistry* **1993**, *32*, 8276–8283.
- Evans, I. P.; Spencer, A.; Wilkinson, G. *Dalton Trans.* **1973**, 204–209.
- Feeney, M. M.; Kelly, J. M.; Tossi, A. B.; Kirsch-De Mesmaeker, A.; Lecomte, J.-P. *J. Photochem. Photobiol., B* **1994**, *23*, 69–78.
- Lentzen, O.; Constant, J.-F.; Defrancq, E.; Prévost, M.; Schumm, S.; Moucheron, C.; Dumy, P.; Kirsch-De Mesmaeker, A. *ChemBioChem* **2003**, *4*, 195–202.
- Matsumura, Y.; Maeda, H. *Cancer Res.* **1986**, *46*, 6387–6392.
- Seymour, L. W.; Duncan, R.; Strohalm, J.; Kopecek, J. *J. Biomed. Mater. Res.* **1987**, *21*, 1341–1358.
- Nogushi, Y.; Wu, J.; Duncan, R.; Strohalm, J.; Ulbrich, K.; Akaike, T.; Maeda, H. *Jpn. J. Cancer. Res.* **1998**, *89*, 307–314.
- Masschelein, A.; Jacquet, L.; Kirsch-De Mesmaeker, A.; Nasielski, J. *Inorg. Chem.* **1990**, *29*, 855–860.
- Lecomte, J.-P.; Kirsch-De Mesmaeker, A.; Kelly, J. M.; Tossi, A. B.; Görner, H. *Photochem. Photobiol.* **1992**, *55*, 681–689.

BM700647B